Synthesis of a Complete Velocity-Temperature Space Mass Transfer Coefficient for Xenon Mass Transfer From The Fuel Salt To The Graphite in the Molten Salt Reactor Experiment

Terry J. Price

March 2018

Itroduction

Molten-Salt Reactors (MSRs) represent on of the GEN IV reactor concepts proposed for development by the Generation IV International Forum (GIF).[1] MSRs circulate a molten alkali fluoride salt with dissolved actinide fuel substances between a graphite moderating region and a heat exchanger. The Molten Salt Reactor Experiment (MSRE) was a molten salt reactor developed and run by Oak Ridge National Laboratory (ORNL) in the 1960s. One of the fission products produced is xenon gas. The neutron poison xenon-135, with its 2.6 Megabarn absorption cross-section, is of particular concern to reactor physics modeling. Xenon-135 is either stored as a dissolved gas in the fuel-salt, or can transfer into circulating voids (bubbles). The xenon dissolved in the fuel-salt may transfer directly from the fuels-salt into the void space of the non-wetted graphite moderator. Due to this transfer process, the xenon concentration in the graphite moderator affects the dynamical xenon behavior of the system.

The transfer of xenon between the graphite and the fuel-salt is determined by the first order equation,

$$\frac{dN_{xe}}{dt} = k_m A \Delta C .$$

Where the concentration differential is between the graphite xenon concentration and the fuel salt xenon concentration. The constant of proportionality for this transfer process is the mass-transfer coefficient (MTC), k_m. Handbooks and data for MTC determination are not as common as for their heat-transfer counterparts, the heat-transfer coefficient (HTC). There are several heat to mass transfer analogies that may be employed to convert heat to mass transfer coefficients,

Both ORNL reports about dynamical xenon behaviour, ORNL-4069 and ORNL-TM-3464, used a temperature and velocity invariant MTCs. [2] [3] This work seeks to expand upon that and develop a MTC for xenon that accounts for both fuel salt velocity and temperature variation for the MSRE.

Prior Work

Prior work on xenon mass-transfer for molten salt reactors is quite limited. Scott and Eatherly state

> "The concentration of xenon in the graphite is controlled by the concentration in the salt, the mass transfer coefficient from the salt to the graphite [this work], the total surface of of graphite exposed to the salt, the diffusion coefficient of the xenon in the graphite, and the void fraction available to xenon. The mass transfer coefficient from the salt to the graphite is very strongly influenced by the characteristics of the salt flow boundary film, together with the area of the graphite exposed to the salt are determined by the heat transfer conditions required to cool the graphite." [4]

As stated in the work by Shimazu, the xenon flux from the graphite is given by

$$\frac{dN_{xe}}{dt}\frac{1}{A}=k_m\left(C_{xe}^{salt}-\frac{HRT}{\epsilon}C_{xe}^{graphite}\right) \quad .$$

The factor HRT/ϵ comes from Henry's law which states that given a system with a gas phase and a liquid phase, and equilibrium conditions, the concentrations of gas in the gas and dissolved in the liquid phase will be related by

$$c_l=hc_g \quad .$$

Where h is the dimensionless Henry's law constant. This dimensionless Henry's law constant cant be related to the pressure based henry's law constant by the expression

$$h=HRT \quad ,$$

for use in the familiar expression,

$$Hp=c_l \quad .$$

The graphite is non-wetted, so the xenon concentration is in the gas phase. Thus, we multiply the graphite xenon concentration by the HRT term gives us the concentration in the liquid phase of the film layer and division by the void fraction reduces the volume of the graphite to that which is just present in the void space of the graphite.

The value of Henry's constant for xenon in molten salts can be found in publications by Grimes, Blander, and Watson. [3] [6] These findings are summarized in the Table 1.

	Temperature [deg. C]	Henry's Law Constant $\times 10^8$ [Moles Xe / (CC. Melt-atm)
NaF-ZrF4 (53-47 Mole %)	600	1.94
	700	3.56
	800	6.32
NaF-ZrF4-UF4 (50-46-4 Mole %)*	600	2.0
	700	4.0
	800	6.5
NaF-KF-LiF (46.5-11.5-42.0 Mole %)	600	0.011
	700	0.057
	800	0.212
LiF-BeF2 (64-36 Mole %)	600	0.88
	700	0.842
	800	0.868

*Table 1: Henry's Law Constant For Xenon in Molten Salt. *Theoretical*

Additionally, ORNL-TM-3464 states that the Henry's law constant for xenon in MSRE fuel-salt is 3×10^{-9} Moles xe / (CC Melt-atm). It ought to be noted that this is a temperature invariant Henry's law constant, but, as can be seen from the table above, Henry's law does indeed vary with temperature.

An expression for the theoretical value of the dimensionless Henry's law constant for gas in a molten salts described by Petrucci,

$$h = \exp\left(-18.08\, r_{gas}^2\, \sigma / RT\right). \quad [7]$$

An expression for the surface tension for various salts can be found in INL/EXT-10-18297.[8]

The MSRE had two distinct operating periods. The first was with U-235 fuel from June 1 1965 to March 26 1968. The second was with U-233 fuel from October 2 1968 to December 12 1969. [9]

The report ORNL-4069 was issued by Kedl and Houtzeel in 1967, midway through the first operational period, and details the development of a model for computing Xe-135 migration in the MSRE. The report describes the so called 'Krypton Experiment' wherein the MSRE was filled with a radioactive krypton-85 gas which saturated the locations in the reactor which could hold krypton (and presumably other gasses such as xenon). After the reactor was saturated with krypton, the krypton supply was cut off and the off gas line of the MSRE was monitored for krypton-85 activity as a function of time. The activity was recorded to produce a curve that describes the krypton-85 activity as function of time. This curve is then descriptive of the rate at which dissolved and entrapped gasses in the reactor system leave the reactor. In particular, the effective release half life of the krypton within the graphite was found to have a half-life of 15.5 hours – a number greater but on the same order of magnitude as Xenon-135's radioactive decay half life of 9.2 hours. Nevertheless, As a result of these experiments, the krypton mass-transfer

coefficient to the bulk graphite of the MSRE was found to be between 0.05 and 0.09 ft/hr. (4.23×10^{-6} and $7.26\times10^{-6} m/s$). Conversely, the center line graphite was found to have a mass transfer coefficient between 0.25 and 0.4 ft/hr (2.12×10^{-5} to 3.4×10^{-5} m/s).

Another aspect of import from ORNL-4069 Krypton Experiment was the determination of the graphite void fraction. ORNL-4069 states " The graphite void fraction came out to be about 0.40. This is obviously incorrect.". The report then goes on to say "[given some corrections to the calculation technique] the result [graphite void fraction] is about 0.04 and this is lower than would be expected. The true void fraction is between the limits of what can be calculated" . This indicates that determination of accessible void fraction to xenon is still an area where research needs to be conducted.

The MTC describes the rate of mass transfer from the bulk fluid to the film interface to the non wetting graphite. Beyond this, there is a region called the pure diffusion region which consists of a graduated concentration of dissolved gas into the pore itself. This is illustrated in the diagram below.

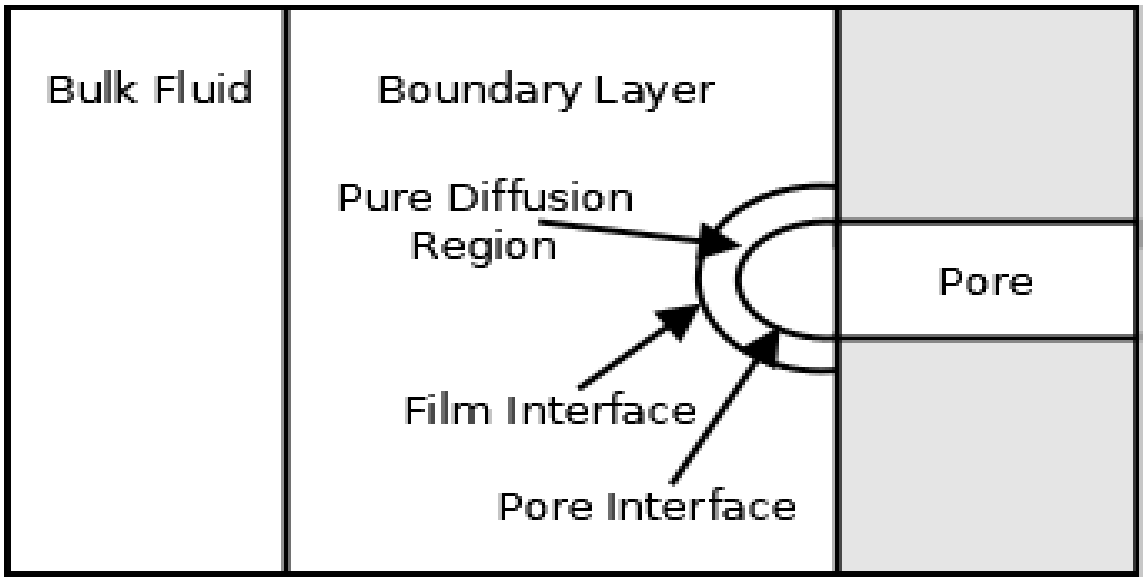

Illustration 1: Pore Interface

If the resistance to mass transfer in this region of pure diffusion is too high, then xenon would accumulate at the surface of graphite and never enter into the bulk of the pores. Annex A of ORNL-4069 modeled this as a hemispheric diffusion problem and showed that the concentration difference between the pore interface and the film interface is negligible compared to the difference in concentration between the film interface and the bulk salt. Since the difference between the concentration between the pure diffusion interface and the film interface is so much smaller than the difference in concentration between the bulk fluid bulk fluid and the film interface, the mass transfer process can be effectively be rewritten as a function of the difference between the bulk fluid and the pore interface rather than a function of difference in concentration between the bulk fluid and the pore interface.

Finally, ORNL-4069 derives mass transfer coeffecients from the Dittus Bottler correlation. This derivation was done with direct replacement of heat transfer quantities with their mass transfer analouges in a manner similar to that which exposited in Bergman's book [9] The results found are shown in table 2.

	Bulk Graphite MTC [m/s]	**Center-Line Graphite MTC [m/s]**
Turbulent Flow	9.8×10^{-6} - 1.3×10^{-5}	2.2×10^{-5} - 2.9×10^{-5}
Laminar Flow	4.1×10^{-6} - 5.7×10^{-6}	-----

Table 2: Mass Transfer Coeffecient Found in ORNL-4069 in [m/s]

It was observed that ORNL-TM-0378 reported MSRE fuel channel Reynolds numbers between 421 and 3150. [10] From these observation, combined with the fact that the Dittus Bottler correlation is only valid for $Re > 10^4$, we can conclude that the Dittus Bottler correlation might not be the most appropriate correlation to use in the MTC prediction for the MSRE.

The 1971 report, ORNL-TM-3464, was released after the operational experience with the MSRE and describes the xenon behavior in the MSRE as well as a mathematical model used to describe the xenon behavior. [3] A parametric study was under taken wherein model parameters were adjusted to fit the observed xenon behavior in the MSRE. A salt to graphite MTC of ($8.47 \times 10^{-7} – 1.52 \times 10^{-5}$ m/s for bulk graphite and $5.08 \times 10^{-6} – 9.65 \times 10^{-5}$ m/s for central graphite was found to fit the data. The only means by which xenon could enter the graphite in the computational model of ORNL-TM-3464 was direct transfer from the liquid. Mass transfer from circulating voids into the graphite was not considered. In analyzing the results of the parametric study, the graphite mass-transfer coeffecient that fit the observed data was lower than that predicted in ORNL-4069 by a factor of 6.

Prior to the work in ORNL-3464, the effects of cover-gas solubility in the fuel-salt were ignored. Observations showed that use of different cover gases in the system produced different fractions of xenon poisoning. That being said, when the parametric studies were performed to match model parameters to results, it was found that in the set of of parameters that matched experimental observation, the mass transfer coefficient to graphite was invariant with respect to cover gas composition.

Finally, the question of the applicablity of heat transfer correlations to molten salt was addressed by the work by Yoder who compared experimental molten salt heat transfer data to predictions by various heat transfer correlations. [12] In particular data were examined from various authors in both natural and forced convection conditions in a circular pipe. Laminar forced convection data were compared to to the Seider Tate correlation,

$$Nu = 1.86\, Pe^{1/3} (D/L)^{1/3} \left(\frac{\mu_b}{\mu_t}\right)^{0.14} .$$

of the turbulent forced convection data Data which were “digitized from a plot of $St^{*Pr^{2/3}}$ vs. Re” were compared to an expression,

$$Nu = 0.023\,\mathrm{Re}^{0.8}\,Pr^{1/3}$$

which similar to the Dittus Boetler correlation,

$$\begin{gathered} Nu = 0.023\,\mathrm{Re}^{4}/5\,Pr^{n} \\ n = 0.4 \rightarrow heating \\ n = 0.3 \rightarrow cooling \end{gathered} \quad .$$

Finally, the turbulent flow data which were not compared to the Dittus Boetler like corelation were compared to the Gnielinski correlation,

$$Nu = \frac{\frac{f_i}{2}\cdot(\mathrm{Re}-1000)\,Pr}{1+12.7\left(\frac{f_i}{2}\right)^{1/2}\left(Pr^{2/3}-1\right)} \quad .$$

$$f_i = \left(1.58\cdot\ln(\mathrm{Re})-3.28\right)^{-2}$$

Yonder’s report concludes

> “The data in the database can be reasonably predicted using conventional heat transfer correlations for common fluids…however, the standard deviation of the heat transfer predictions is relatively large….this is particularly true at lower Reynolds numbers (<~40,000)”.

However, he also warns,

> “The accuracy of the heat transfer analysis depends of the accuracy of the properties being analyzed. Historically, errors in the properties have led to conflicting or erroneous conclusions regarding the data.”.

Thus, in conclusion, solubility data of xenon in molten salts has been looked into by various authors. The mass transfer rate of xenon from and into graphite is determined by a straight forward first dimensional ordinary differential equation. The Oak Ridge reports examined various aspects of xenon mass transfer into graphite including experimental measurements of Xenon mass transfer rates, determination of mass transfer coefficients from heat transfer coefficients, an examination of mass transfer past the film layer into the pore interface, and comparison of graphite xenon mass transfer coefficients to experimental values. Finally, heat transfer correlations have been compared to experimental data and justification has been found for using various heat transfer correlations in molten-salt data. Non of the prior work generated MSRE xenon MTC as a function of fuel salt velocity or temperature, and it is here that our work enters.

Methodology

Overview

This work developed a system that predicts mass transfer coefficients for the MSRE in the velocity-temperature domain [0,3] m/s × [750,1850] K. This velocity-temperature domain will be henceforth refered to as UT space. Three methods were used to determine the MTC in this space: Chilton-Coulburn J-Factor, Friend-Metzner, and direct replacement. More information on both the Chilton-Coulborn and Friend-Metzner analogies is detailed in the book by Brodkey.[13] The direct replacement technique was used in ORNL-4069, and is detailed in Bergman's book. [2], [10] The Chilton-Coulborn analogy is valid for $Re > 10^{4.}$. The Friend-Metzner analogy is valid for $0.5 < Sc < 3000$. No literature was found on the validity of direct replacement, and, as such, will only be used in regions where neither the Friend-Metzner analogy nor the Chilton-Coulborn analogies are applicable.

Many of the correlations used in this work require the mass diffusion coefficient to be used in their evaluation. This was done with the Einstien-Stokes equation,

$$D = \frac{K_b T}{6 \pi \mu(T) r_{xe}} \quad ,$$

which gives the mass diffusion coeffecient for a spherical particle immersed in a liquid. [14]The temperature is taken to be the bulk fuel-salt temperature. The radius of xenon used corresponds to the Xenon van der Waals radius of 216 angstrom, since, by definition, the van der Waals radius is that of of conceptually hard sphere atom, and the Einstien-Stokes equation also conceptualizes that the diffusing particle is a hard sphere. The validity of applying the Einstien Stokes equation to molten salts is discussed by Brockis and Reddy. [15]

The domain of potential temperatures is evaluated from 750-1850 K whereas the domain of potential velocities ranges from 0-3 m/s. The space of potential velocities and temperatures at which the heat transfer coefficient will be evaluated is referred to as the UT (velocity-temperature) space.

The Chilton-Couborn analogy is stated as,

$$\frac{f}{2} = j_H = j_M ,$$

where ,

$$j_M = St_M Sc^{2/3} ,$$

and,

$$j_H = St_H Pr^{2/3} \quad .$$

Expressions for the mass-transfer coefficients can be found as functions of heat-transfer parameters and fanning friction parameters.

$$k_m = \frac{f}{2} * \mathrm{Re}\, Sc^{1/3} \frac{D}{L}, \tag{1}$$

And,

$$k_m = \frac{h}{k}\left(\frac{Sc}{Pr}\right)^{1/3} D. \tag{2}$$

The fanning fiction factor may be determined by the Churchill correlation, which covers the full range of laminar and turbulent flows.,

$$f(u,T) = 2\left(\left(\frac{8}{\mathrm{Re(u,T)}}\right)^{12} + \left(A(u,T) + B(u,T)\right)^{-1.5}\right)^{1/12}$$
$$A(u,T) = \left(2.457 \ln\left(\left(\frac{7}{\mathrm{Re(u,T)}}\right)^{0.9} + 0.27\frac{\epsilon_r}{L}\right)^{-1}\right)^{16} \qquad [16]$$
$$B(u,T) = \left(\frac{36530}{\mathrm{Re}(u,T)}\right)^{16}$$

Three heat transfer correlations were used to fill the entirety of the UT space. The reader is refered to Tosun for a descrption of these correlations. [17] The first heat transfer correlation is the Sieder Tate correlation for laminar flow,

$$h_1(u, T_{bulk}, T_{wall}) = 1.86\left(\mathrm{Re}(u, T_{bulk})\,\mathrm{Pr}(T_{bulk})\frac{L}{H}\right)^{1/3}\left(\frac{\mu(T_{bulk})}{\mu(T_{wall})}\right)^{0.14}\frac{k}{L} \tag{3}$$

Which is valid in the region 13 < Re <2030. The next correlation is the Whitaker correlation,

$$h_2(u, T_{bulk}, T_{wall}) = 0.015\,\mathrm{Re}(u, T_{bulk})^{0.83} Pr(T_{bulk})^{0.42}\left(\frac{\mu(T_{bulk})}{\mu(T_{wall})}\right)^{0.14}\frac{k}{L} \tag{4}$$

.

Which is valid between 2300 < Re < $1\times10^{5;}$ however, it is only used up to Re < 1×10^4. For the region above Re > 1×10^4, the Dittus Boelter equation is used,

$$h_3(u, T_{bulk}) = 0.023\,\mathrm{Re}(u, T_{bulk})^{4/5} Pr(T_{bulk})^n \frac{k}{L} \quad . \tag{5}$$

Where n is 0.4 if heating, and 0.3 for cooling. A special case where the bulk temperature is the same as the wall temperature is defined such that n=0.35, and this is justified on the fact that Yoder's Dittus Boetler like equation with its n of 1/3 was deemed in good alignment with the experimental data. [12]

The bulk and wall temperatures were taken to be the same in these each of these correlations. This is justified on two points: The first point is as follows:: In all of the previously mentioned correlations, the only place that the difference in bulk and wall temperatures is used is in the ratio of wall to bulk viscosity. In these correlations, the ratio of bulk to wall viscosity is raised to an exponent of 0.14. The exponent of 0.14 is the smallest exponent on any of the factors in any of the correlations. It follows that the sensitivity of the heat transfer coefficient to variation in the bulk to wall viscosity is smaller than any of the other factors in each of the correlations. The second point is that the temperature of the graphite and the bulk fluid are coupled and near each other in magnitude. In ORNL-TM-0378, the difference in steady state central core fuel salt and graphite temperature was 33 K.[11] Furthermore, the 33 K figure in ORNL-TM-0378 is the bulk graphite temperature, and the wall temperature, as the surface of the bulk temperature, can be expected to be even closer to the bulk fluid temperature. So, given that there is expected to a low sensitivity to changes between bulk and wall temperatures, and the wall and bulk temperatures are coupled. The entire factor,

$$\left(\frac{\mu(T_{bulk})}{\mu(T_{wall})}\right)^{0.14,}$$

is set to unity. The utility in this is that the entire UT field can be evaluated in terms of a single temperature and velocity parameter.

The Friend-Metzner analogy is stated as,

$$k_m = \frac{f/2}{1.20 + (11.8)(f/2)^{1/2}(Sc-1)(Sc)^{-1/3}} \mathrm{Re}\, Sc \frac{D}{L} \quad .$$

The Friend-Metzner analogy is used under the consideration, that at high Schmidt numbers, the difference between experimental and predicted values may be as large as 35%. [13]

For direct replacement, the heat transfer correlations mentioned above had their Prandtl number replaced with Schmidt numbers, their thermal conductivity replaced with mass diffusion. They are,

$$k_{m1}(u,T) = 1.86\left(\mathrm{Re(u,T)}\,\mathrm{Sc(T)}\frac{L}{H}\right)^{1/3}\frac{D(T)}{L} \quad , \tag{6}$$

$$k_{m2} = 0.015\,\mathrm{Re(u,T)}^{0.83}\,Sc(T)^{0.42}\frac{D(T)}{L} \quad , \tag{7}$$

$$k_{m3} = 0.023\,\mathrm{Re(u,T)}^{4/5}\,Sc(T)^{1/3}\,\frac{D(T)}{L} \quad . \tag{8}$$

For the Chilton-Coulborn analogy, two sub maps needed to be created, one for the fanning friction factor and another for the heat transfer coefficient. The first sub map was based on the Fanning friction factor. The Churchill correlation was evaluated at each point in UT space, and fed into equation 1 which was also evaluated at every point in UT space. For the second sub map, based in the heat transfer coefficient, the applicability of equations 3, 4, and 5 were evaluated at every point in UT space. For regions where no HTC was found to be applicable, the unmarked region was filled in with the value the nearest region with a HTC applicable. The filled in HTC space has jump discontinuities due to the different heat transfer correlations used. The entire HTC map was treated as a scalar field and the diffusion equation was solved on it with zero-flux Neuman boundary conditions. A diffusion coefficient of 0.02 was used, and the solution time was for 3 seconds. This reduced the maximum Laplacian of the HTC map from 10348 to 31 while only changing the mean value of the HTC map relatively unchanged.

The Friend Metzner correlation was likewise evaluated at every point in UT space. The Fanning friction factor used in the Friend-Metzner correlation was evaluated in the same manner as before from the Churchill correlation.

Finally, for the direct replacement technique, the applicability of equations 6, 7, and 8 were evaluated at every point in UT space. The regions of UT space that had no applicable direct replacement derived MTC were filled with their nearest neighbor. Again, the jump discontintuues were eliminated by treating the entire direct replacement MTC map as a scalar field and the diffusion equation was solved on it for 3 seconds, with a diffusion coeffecient of 0.02, and Neuman, zero-flux boundary conditions.

The entirety of UT space, as frame 2 illustrates, was then demarcated according to the applicability of each mass transfer analogy. There is some overlap between the regions of applicability between direct replacement, Friend Metzner, and Chilton-Coulborn J-Factor. This discrepancy between the regions of applicability was solved by setting the precedence of applicability of the three different mass transfer analogies to Chilton-Coulborn J-Factor, followed by Friend-Metzner, followed by direct replacement.

Each point in UT space then had the correspondent MTC from the analogy as indicated by its demarcation copied over to it to generate the complete MTC map. This final MTC map was then smoothed by treating it as a field of scalar quantities which was set as the initial condition in the diffusion equation with Neuman, zero-flux boundary conditions. The diffusion equation was solved with a diffusion coefficient of 0.03 for 3 seconds. The final result was used as the MTC map.

Validation

The MTC generated in this paper is to be compared to that which was generated for the MSRE as described in ORNL-TM-3464. [3] ORNL-TM-3464 makes mention of a parametric studies in which their MSRE xenon model had its parameters chosen in such a way that the predicted xenon poisoning

produced by the xenon model fit the observations from the MSRE xenon observations. The table below summarizes the fuel salt to graphite mass transfer coefficients reported in ORNL-TM-3464.

Region Description in ORNL-4069	Value [m/s]
'Most Graphite'	8.47×10^{-7}
'Central Region	5.33×10^{-6}

The predicted mass transfer coefficients are generated as a function of core region as per the discretization in ORNL-TM-0378.

In order for the MSRE fuel channel to be recreated, several items of data will be needed. ORNL-TM-0728 provides details about the fuel channel dimensions. Fuel channels measure 3.048 × 1.016 cm and have circularly rounded corners. The fuel channel geometry, as depicted in figure 5.7 of ORNL-TM-0728, may be decomposed into 1 rectangle measuring 2.54 ×1.016 cm, and two half circles, each with radii of 0.51 cm. The two half circles are located at the ends of the rectangle. Conceptualizing the geometry as such, the total cross sectional area of a fuel channel is 3.39 cm^2 and there is a perimeter of 10.30 cm. These values give an equivalent hydraulic diameter of 1.32 cm for the MSRE fuel channel.

The variation in fuel-salt thermophysical properties with respect to temperature are not given in the MSRE design report, ORNL-TM-0728; however, a database of temperature dependent thermophysical properties is given in ORNL-2316 (edited by S. Cantor).[7] The fuel salts in ORNL-2316 are denoted F_1-F_4, and each of them have a unique composition. There is an issue, however, in using ORNL-TM-2316 data in that none of the salt mixtures given are identical in composition to the MSRE fuel salt as outlined in ORNL-TM-0728. This discrepancy is solved by choosing fuel salt F_4 in ORNL-2316 to act as an analogue to the MSRE fuel-salt. Justification for this choice will be made by considering the compositions of fuel salt and comparing them to the MSRE fuel salt composition. Under this consideration, in terms of LiF and BeF_2 fractions, the composition of salt F_4 is closest, to the partially enriched MSRE fuel salt. Furthermore, since the LiF and BeF_2 fractions are the two most significant components of the fuel salt, and as such, the influence of other constituent components are not considered in the determination of the most appropriate analogue.

Another property, the viscosity, as stated in ORNL-TM-2316, of fuel salt F_4 is given by the expression,

$$\mu(T)[kg/m\text{-}s] = (4.44 \times 10^{-5}) \cdot \exp\left(\frac{2086.11}{-255\,T[K]}\right) \quad .$$

The specific heat at constant pressure is invariant for the liquid phase of fuel salt F_4 and is cited as 1381 J/kg-K. The liquid density is given by the expression,

$$\rho(T)[kg/m^3] = 3933 - 1.134 \cdot T[K] \quad .$$

The thermal conductivity for F_4 is 0.7 W/m-K and has negligible temperature dependence as justified by the statement,

> "As a first approximation, the temperature dependence of thermal conductivity may be neglected. Although the thermal conductivity of molten salts does vary somewhat with temperature, uncertainties in measurements at a given temperature are usually greater than the temperature dependence over the whole range of temperature.".

The final piece of information used in the validation of the presented technique is the height of the fuel channels. This data is found in ORNL-TM-0728, and is stated as 67" (1.7 m).

Finally, the temperature and velocity at which the MTC is to be generated are needed. According to ORNL-TM-0378, the MSRE had a maximum mid plane fuel salt temperature of 933K and a minimum mid-plane fuel salt temperature of 917K. Furthermore, ORNL-TM-0378 subdivides the MSRE fuel channels into 5 flow regions, summarized in the table below.

Region	Velocity [m/s]
1	0.666
2	0.201
3	0.499
4	0.274
5	0.088

Region 5 will be ignored since it is the annular region between the moderator and the reactor shell. Therefore MTCs shall be generated for velocities that correspond regions 1-4 at temperatures of 917 and 933K.

Results and Discussion

Frame 3 shows the delineation of the differentiate mass transfer analogies. Frame 4 shows the resultant mass transfer coefficient map generated. Frame 5 shows the absolute value of the laplacian of the mass transfer coefficient map. Frame 6 shows the mass transfer calculated by this method for each of the regions mentioned in ORNL-TM-0378. It was found that the 'most' graphiteMTC is lower than all the calculated values whereas the 'central' graphite MTC is higher than all of the calculated values.

Conclusion

MTCs for xenon mass transfer between fuel salt and graphite for an expected range of temperatures and fuel salt velocities in the MSRE. The full range of potential velocities and temperatures required three different techniques to generate MTCs. When compared to MTCs that fit experimental data, the MTCs were between the upper and lower bounds of the values as presented in ORNL-TM-3464.

Bibliography

[1]. U.S. Department of Energy and Generation IV International Forum, *GIF-002-00: U.S. Department of Energy and Generation IV International Forum*. Generation IV International Forum, 2002.

[2]..R. Kedl and A. Houtzeel, *ORNL-4069: Developent of a Model for Computing Xe-135 Migration in the MSRE*. Oak Ridge National Laboratory, 1967.
[3] J. Engel and R. Steffy, *ORNL-TM-3464: Xenon Behavior in the Molten Salt Reactor Experiment*. Oak Ridge National Laboratory, 1971.
[4] D. Scott and W. Eatherly, “Graphite and Xenon behavior and their influence on molten-salt reactor design,” *Nucl. Appl. Technol.*, vol. 8, no. 2, pp. 179–189, 1970.
[5]W. Grimes, N. Smith, and G. Watson, “Solubility of Noble Gases in Molten Fluorides. I. In Mixtures of NaF–ZrF4 (53–47 Mole%) and NaF–ZrF4–UF4 (50–46–4 Mole%),” *J. Phys. Chem.*, vol. 62, no. 7, pp. 862–866, 1958.
[6] M. Blander, W. Grimes, N. Smith, and G. Watson, “Solubility of Noble Gases in Molten Fluorides. II. In the Lif–NaF–LF Eutectic Mixtures,” *J. Phys. Chem.*, vol. 63, no. 7, pp. 1164–1167, 1959.
[7] S. Petrucci, *Ionic Interactions: From Dilute Solution to Fused Salts*. Elsevier Science, 2012.
[8] T. Allen, “Molten salt Database,” *Nucl. Eng. Eng. Phys. Dep. Univ. Wis.*
[9] C. Forsberg, “Molten Salt Reactor Experience Applicable to LS-VHTR Refueling,” presented at the LS-VHTR Meeting, Germantwon, Maryland, 2006.
[10] T. L. Bergman, F. P. Incropera, D. P. DeWitt, and A. S. Lavine, *Fundamentals of Heat and Mass Transfer*. Wiley, 2011.
[11] J. Engel and P. Haubenreich, “ORNL-TM-378: Temperature in the MSRE Core During Steady-State Power Operation,” Oak Ridge National Laboratory (ORNL), Oak Ridge, TN (United States).
[12] G. L. Yoder Jr, “Examination of Liquid Fluoride Salt Heat Transfer,” in *International Congress on Advances in Nuclear Power Plants (ICAPP), Charlotte, NC, Apr*, 2014, pp. 6–9.
[13] R. S. Brodkey and H. C. Hershey, *Transport Phenomena: A Unified Approach*. Brodkey Pub., 2003.
[14] E. L. Cussler, *Diffusion: Mass Transfer in Fluid Systems*. Cambridge University Press, 2009.
[15] J. Bockris and A. Reddy, *Volume 1: Modern Electrochemistry: Ionics*. Springer US, 1998.
[16] S. W. Churchill, “Friction-factor equation spans all fluid-flow regimes,” *Chem. Eng.*, vol. 84, no. 24, pp. 91–92, 1977.
[17] I. Tosun, *Modeling in Transport Phenomena: A Conceptual Approach*. Elsevier Science, 2007.
[18]. S. Cantor, *ORNL-TM-2316: Physical Properties of Molten-Salt Reactor Fuel, Coolant, and Flush Salts*. Oak Ridge National Laboratory, 1968.